



## Influence of mechanical stratigraphy and kinematics on fault scaling relations

MICHAEL R. GROSS\*

Department of Geology, Florida International University, Miami, FL 33199, U.S.A.

GABRIEL GUTIÉRREZ-ALONSO

Departamento de Geología, Universidad de Salamanca, 37008 Salamanca, Spain

TAIXU BAI, MICHAEL A. WACKER and KEVIN B. COLLINSWORTH

Department of Geology, Florida International University, Miami, FL 33199, U.S.A.

and

RICHARD J. BEHL

Department of Geological Sciences, California State University, Long Beach, CA 90840, U.S.A.

(Received 19 February 1996; accepted in revised form 30 September 1996)

**Abstract**—In order to document effects of mechanical anisotropy, fault geometry, and structural style on displacement–length ( $D$ – $L$ ) scaling relations, we investigated fault dimensions in the lithologically heterogeneous Monterey Formation exposed along Arroyo Burro Beach, California. The faults, which range in length from several centimeters to several meters, group into two populations: small faults confined to individual mudstone beds, and larger faults that displace multiple beds and often merge into bedding plane detachments. Whereas a linear correlation exists between displacement and length for small faults, displacement across large faults is independent of length. We attribute this deviation from scale-invariance to a combination of geologic factors that influence fault growth once faults extend beyond the confines of mudstone beds. Propagation of large faults across higher moduli opal-CT porcellanite leads to a reduction in  $D/L$ , as does the development of drag folds. Further scatter in  $D/L$  occurs when fault tips splay as they approach detachments. Large faults eventually merge into bedding plane detachments, which originally formed due to flexural slip folding. Extremely high  $D/L$  ratios are recorded for these merged faults as they accommodate block rotation within a simple shear zone. Thus, both mechanical stratigraphy and the temporal evolution of fault systems can lead to a breakdown in fault scaling relations thought to characterize isolated fault growth in a homogeneous medium. © 1997 Elsevier Science Ltd. All rights reserved

### INTRODUCTION

Relations among fault parameters such as length, width, displacement, and gouge thickness have been the focus of considerable attention over the past 20 years (e.g. Elliott, 1976; Hull, 1988; Clark and Cox, 1996). Knowledge of fault dimensions, in turn, provides valuable constraints on a number of geologic applications such as calculating seismic and geometric moments (Marrett and Allmendinger, 1991), estimating strain in a region (Scholz and Cowie, 1990; Walsh *et al.*, 1991; Marrett and Allmendinger, 1992) and developing models for fault growth (Walsh and Watterson, 1988; Cowie and Scholz, 1992a; Cladouhos and Marrett, 1996).

One well-established relationship is the correlation between fault length (and width) and displacement, which follows the general formula  $D \propto L^n$ , where  $L$  is fault length,  $D$  is maximum displacement across the fault, and  $n$  is the power law exponent (e.g. Muraoka and

Kamata, 1983; Cowie and Scholz, 1992b; Gillespie *et al.*, 1992; Dawers *et al.*, 1993). The global data set, which includes faults ranging from outcrop (m) to seismic (km) scale, was recently augmented by displacements measured across small faults having 1–14 cm lengths (Schlische *et al.*, 1996). Although the precise value of  $n$  remains the subject of debate, combined data sets spanning more than eight orders of magnitude reveal a general trend that maximum displacement across a fault does indeed scale with fault length.

Inspection of global fault data sets, however, reveals a large degree of scatter partially masked by the nature of log–log plots (refer to plots in Marrett and Allmendinger, 1991; Gillespie *et al.*, 1992; Schlische *et al.*, 1996). Factors in addition to measurement errors and outcrop limitations may be responsible for this scatter. Cowie and Scholz (1992b) question the validity of combining fault data from different lithologies and tectonic settings on theoretical grounds because fault growth may depend upon material properties and loading conditions. Peacock and Sanderson (1991) and Dawers and Anders (1995) show that  $D/L$  ratios may be higher in areas of

\*Author to whom correspondence should be addressed. Fax: 305-348 3877; E-mail: Grossm@servax.fiu.edu

overlapping fault segments and splays, and Cartwright *et al.* (1995) suggest that linkage of fault segments is a primary reason for the observed wide scatter in displacement versus fault length. Numerical models of Bürgmann *et al.* (1994) suggest that mechanical anisotropy and overlapping fault tips can profoundly impact  $D/L$  ratios, while field observations by Wojtal (1994, 1996) reveal different displacement population coefficients for faults of different sizes, attributed to changes in structural style during temporal evolution of fault systems. Thus, a host of geologic scenarios may lead to deviations from an idealized universal scaling law for fault dimensions.

The purpose of our field study is to investigate the effects of mechanical stratigraphy (i.e. variations in mechanical properties that result from changes in lithology or the presence of structural discontinuities; Gross, 1995) and fault kinematics on displacement-length scaling relations. By selecting an outcrop with diverse lithology and a deformation history that can be traced through time, we hope to isolate individual factors that may impact the magnitude of displacement across faults. These factors include mechanical properties, frictional drag, fault termination geometry, and the merging of faults into bedding plane detachments.

## GEOLOGIC SETTING

Geometries and dimensions of normal faults were investigated in the Miocene Monterey Formation exposed along Arroyo Burro Beach in Santa Barbara, California (Fig. 1). The section is located in the southern flank of the western Transverse Ranges, a crustal block situated west of the San Andreas fault that has undergone  $\sim 90^\circ$  of clockwise rotation since the middle Miocene (e.g. Crouch, 1979; Luyendyk *et al.*, 1985; Hornafius, 1985). Presently the western Transverse Ranges are an actively developing fold and thrust belt, with NNE–SSW oriented contraction manifested by detachment and fault-related folding (Yeats, 1983; Namson and Davis, 1988; Shaw and Suppe, 1994). The switch in regional tectonic regimes during the early Pliocene from block rotation about a vertical axis accommodated by mainly strike-slip faulting to contractional folding and thrust faulting resulted in generally EW-trending, strike-parallel extension. In mudstone lithologies at Arroyo Burro, this Pliocene–Holocene along-strike extension is accommodated by normal faulting (Gross and Engelder, 1995).

The Monterey Formation was deposited in a series of deep anoxic basins along the California borderland during the middle to late Miocene (Isaacs, 1980; Pisciotto and Garrison, 1981). It consists of interbedded limestones, dolostones, mudstones, shales, and silica-rich horizons. The dominant source of silica in the Monterey Formation was biogenic. Under increasing burial depths and temperatures, siliceous beds, originally composed of diatom frustules in the form of amorphous opal A, are

diagenetically converted to an intermediate though unstable opal-CT phase. Further increases in temperature result in transformation from opal-CT to the stable diagenetic quartz phase (Bramlette, 1946; Murata and Larson, 1975). Diagenesis is also affected by silica purity, such that adjacent beds of different compositions may be at different stages of silica diagenesis (Isaacs, 1982).

The main mechanism accommodating shortening at Arroyo Burro is multi-layer flexural-slip folding with shear displacement concentrated along numerous thin clay horizons (Fig. 1c). Tangential longitudinal strain occurs within individual layers. Folds at Arroyo Burro are cylindrical with NW–SE-trending horizontal to subhorizontal axes. The study site, referred to as 'Station A', is located on the NE-dipping limb of a small ( $\sim 200$  m wavelength) anticline within the Carbonaceous Marl Member of the Monterey Formation. At this locality the Carbonaceous Marl Member consists of organic and phosphatic-rich calcareous mudstones interbedded with clays, dolostones and opal-CT porcellanites (Isaacs, 1983). The wide range in lithologies, and hence mechanical properties, results in fracture partitioning, with mode-I joints and veins restricted to pure dolostone and siliceous beds and normal faults generally confined to mudstone horizons (Gross, 1995). The measured faults are confined to a composite mechanical unit 3.3 m thick consisting of alternating organic-rich mudstone, calcareous mudstone, calcareous opal-CT porcellanite, and pure opal-CT porcellanite. The unit, bounded above and below by thin clay detachment horizons, is subdivided into 19 lithologic beds (Fig. 2). A cross-section sketch of Station A shows the distribution of faults with respect to mechanical stratigraphy (Fig. 3).

## NORMAL FAULTS

Normal faults at Arroyo Burro group into two main categories based on trace length: small faults less than 70 cm in length restricted to individual beds, and large faults between 0.9 and 2.6 m that extend across multiple beds. The large faults cut through numerous opal-CT beds and may contain gouge and/or deformed wall rock up to 17 cm in thickness. Within large fault zones, polyhedral pieces of opal-CT are preserved due to their competent behavior, while mudstone tends to stretch and flow in a ductile manner. Tips of the large faults often merge into bedding plane detachments, or break down into numerous splays as they approach detachments or other large faults (Fig. 3). In contrast, most of the small faults are confined to phosphatic mudstone intervals, and do not extend into neighboring opal-CT beds. Thus, maximum length of small faults is restricted by the stratigraphic distance between bounding opal-CT horizons, with small faults found primarily in mudstone beds #5, #7, #10, #12–14, and #16–18 (Fig. 2).

Orientations of large and small faults cluster into similar conjugate pairs, with mean orientations of

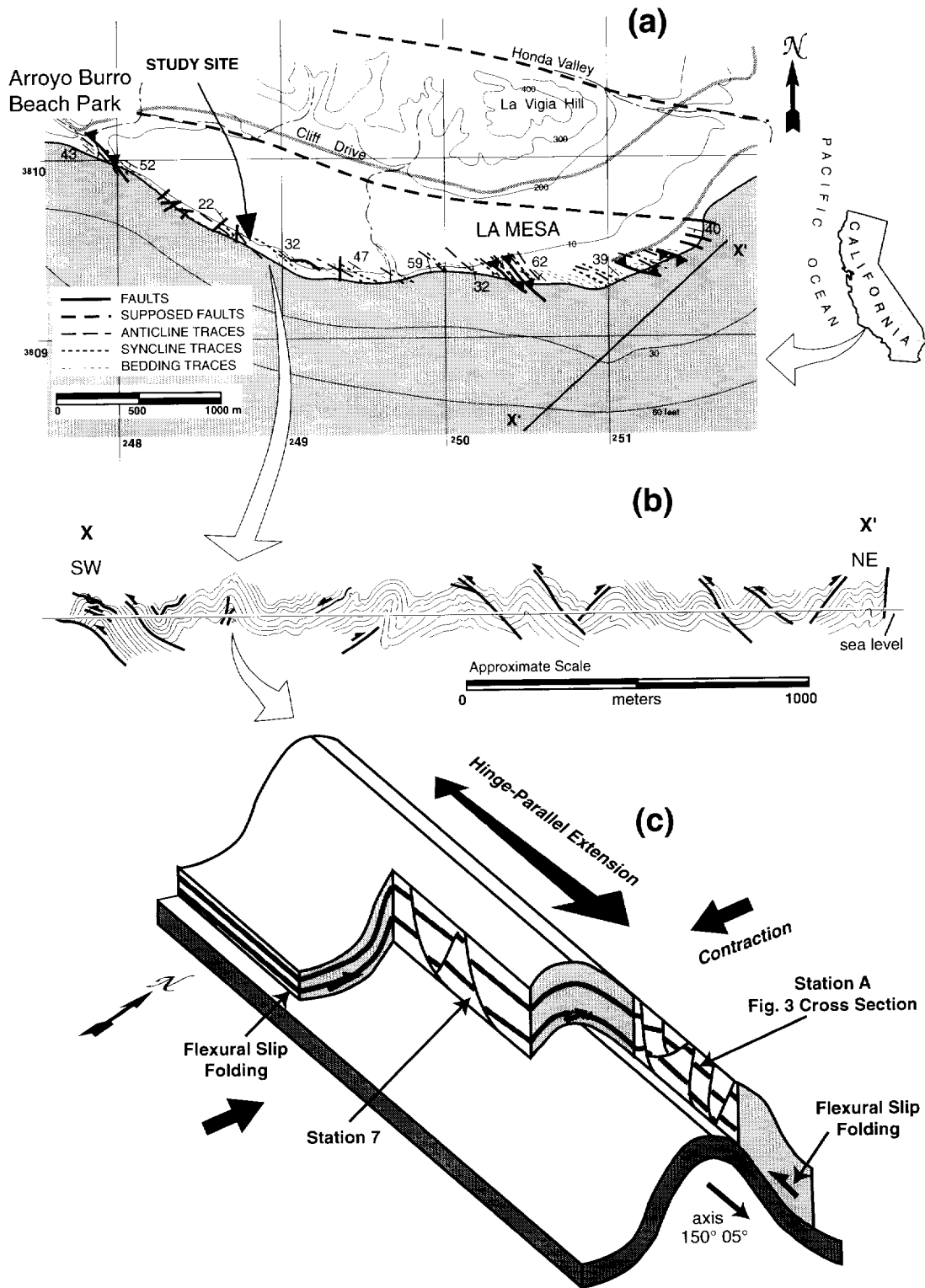


Fig. 1. (a) Map of structures along Arroyo Burro Beach, Santa Barbara, California. Note the consistent NW-SE-trending thrust faults and fold axes. (b) Projected X-X' cross-section for Arroyo Burro Beach, demonstrating NE-SW contraction characterized by fault-related folding. (c) Schematic representation of structural position of studied normal faults. The faults, found on opposing flanks of a flexural slip anticline, accommodate extension parallel to the fold hinge.

~244° 67° NW and ~039° 67° SE (Fig. 4). Thus, faults at different scales most likely formed coevally under the same tectonic stress regime. Slickensides are not preserved on fault surfaces, though fold axes of cylindrically dragged opal-CT layers adjacent to large faults serve as

excellent kinematic indicators of pure dip-slip motion. In addition, the fact that the number of faults dip equally in both directions implies a pure shear origin with maximum principal stress as the acute bisector of mean fault planes. Extensional faults are among the latest structural

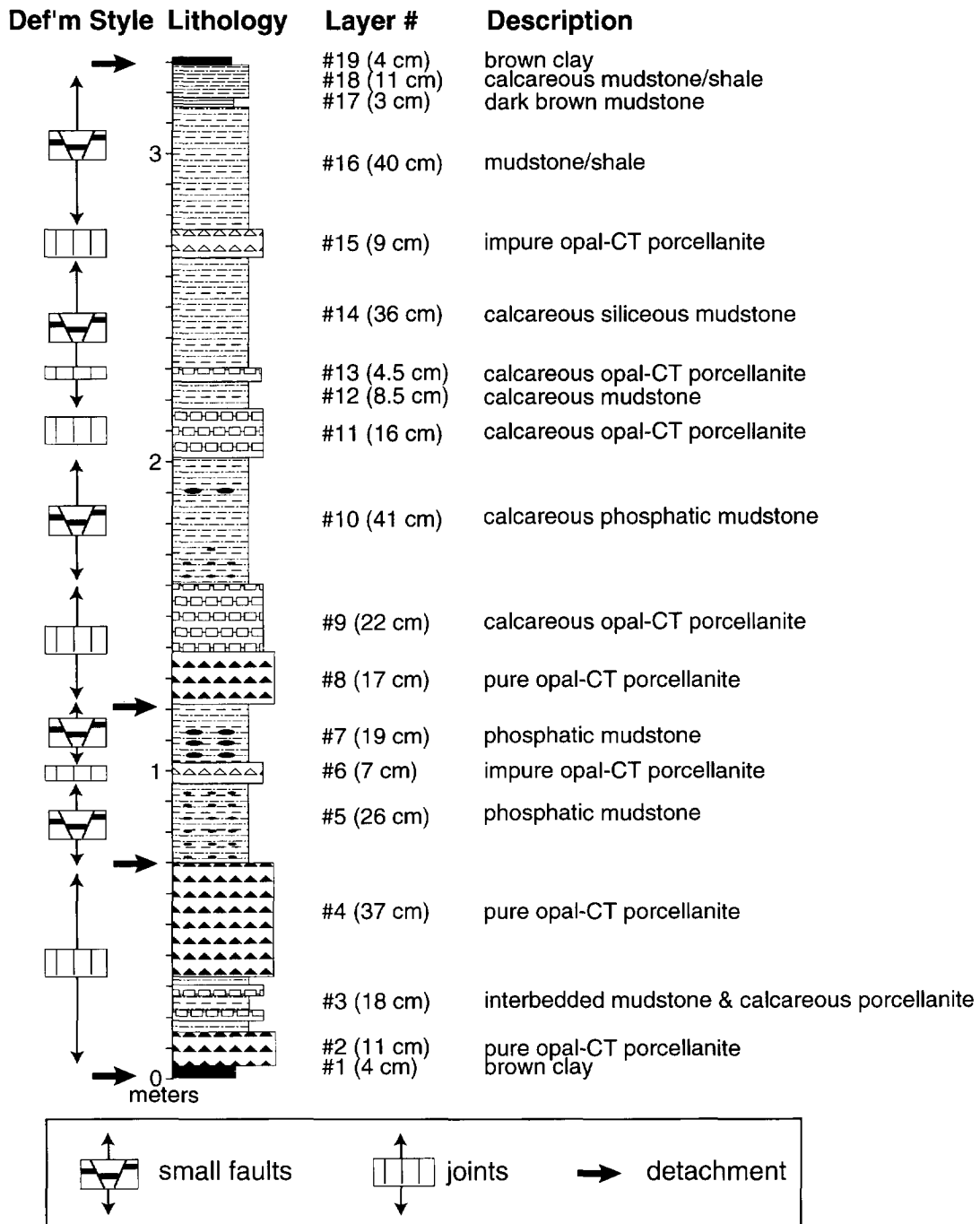


Fig. 2. Mechanical stratigraphy for the section of Monterey Formation exposed at Station A. Small normal faults are mostly confined to mudstone beds, whereas jointing is the dominant style of brittle deformation in opal-CT porcellanite beds.

features to form at Arroyo Burro (Gross, 1995; Gross and Engelder, 1995), and display no evidence for subsequent reactivation.

Fault dimensions and geometries such as orientation, maximum dip separation, trace length, gouge/fill thickness, nature of termination, and cut-off lines were measured and described for the normal faults exposed at Arroyo Burro Beach. We define fault length according to the terminology of Walsh and Watterson (1988), who refer to fault length ( $L$ ) as the maximum fault surface dimension parallel to slip direction, and fault width ( $W$ )

as the maximum dimension normal to slip direction. The outcrop face at Station A, oriented normal to fault strike, provides a continuous exposure of stratigraphy and fault traces for more than 50 m. Numerous thin (mm–cm) laminations in mudstones as well as uniformly thick opal-CT horizons serve as excellent markers for measuring dip separation. We measured dimensions of small faults with a vernier caliper, which provided estimated measurement errors of  $\pm 0.2$  cm for offsets and  $\pm 1.0$  cm for lengths. We estimate measurement errors for large faults of  $\pm 1.0$  cm for offsets and  $\pm 5.0$  cm for lengths. Because

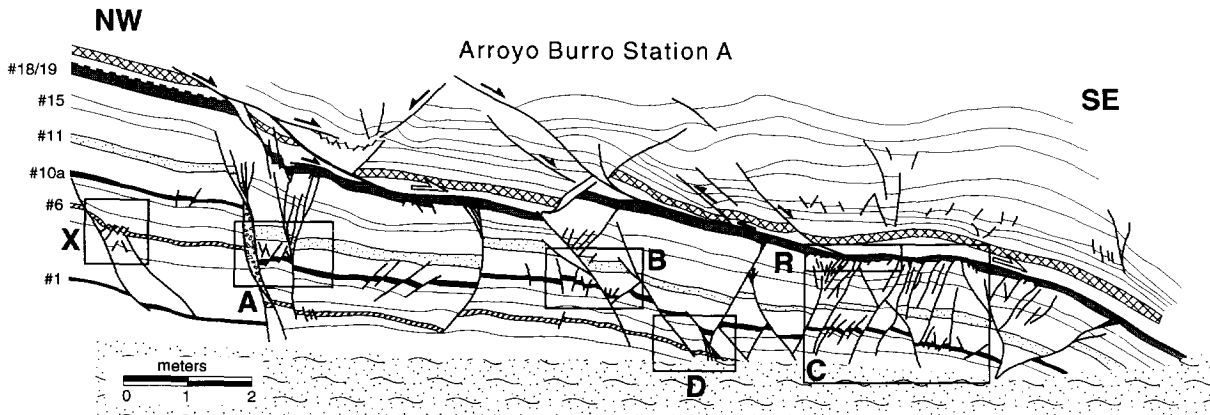


Fig. 3. Cross-section of Section A showing distribution and geometry of normal faults. The measured faults are found beneath the main detachment (bed #19). Selected marker horizons are numbered according to the stratigraphic section in Fig. 2. Labeled boxes represent areas of small fault measurements.

motion on normal faults was dip-slip without subsequent reactivation, and the outcrop is oriented normal to fault strike, we infer that dip separation is nearly equal to true displacement across the faults (Wojtal, 1996).

A total of 18 large faults were encountered at Station A (Fig. 3), although accurate lengths were attainable for only 15 due to outcrop limitations. Therefore, in order to augment the data set for large faults, 10 normal faults

belonging to the same population from a similar mechanical unit on the SW-dipping limb of the anticline were incorporated into the study (Fig. 1c). Details of this latter section (Station 7) may be found in Gross and Engelder (1995). Small faults were measured at six localities along the section (labeled A, B, C, D, R, and X in Fig. 3). Examples of small faults, which range in length from 1.0 to 70 cm, are shown in photographs and sketches of Sections A and C (Figs 5 & 6). Although the entire Monterey Formation section at Arroyo Burro is intensely fractured, small faults are generally restricted to mudstone lithologies (layers #10, #15, #17 in Figs 5 and 6); prominent closely-spaced fractures in the opal-CT beds are mostly opening-mode joints and veins. Substantial offset of opal-CT layers (e.g. #11, #13, #15) occurs mainly across large faults (Figs 3, 5 & 6).

The development of extensional faults at Arroyo Burro occurred in conjunction with local folding, both in response to Pliocene–Holocene tectonic contraction. Simple shear concentrated along thin clay horizons during flexural slip folding, while intervening rock units extended along strike under a pure shear regime. The latter deformation was accomplished by the propagation of opening-mode veins in dolostones and porcellanites while normal faulting predominated in mudstones (Gross, 1995; Gross and Engelder, 1995). Sibson (1996) describes the resulting outcrop fracture pattern as belonging to a ‘Hill-type’ fault–fracture mesh. The normal faults initiated as conjugate pairs within individual mudstone beds. As time progressed and tectonic contraction intensified, a number of normal faults extended beyond the confines of individual mudstone beds, cutting across more competent opal-CT layers. Some of the faults eventually merged into the bedding plane detachments, whereas others terminated prior to reaching these surfaces of flexural slip. Upon merging into detachments, fault-bounded blocks became free to rotate as displacements across large faults were transferred to the bedding plane slip horizons.

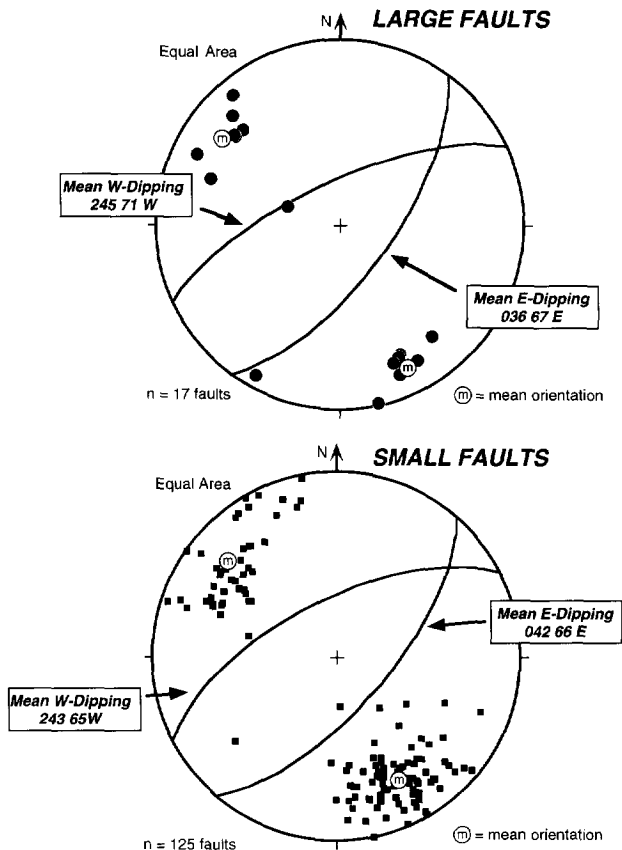


Fig. 4. Lower hemisphere stereoplots of poles to fault planes at Station A. Note that large and small faults group into similar conjugate sets.

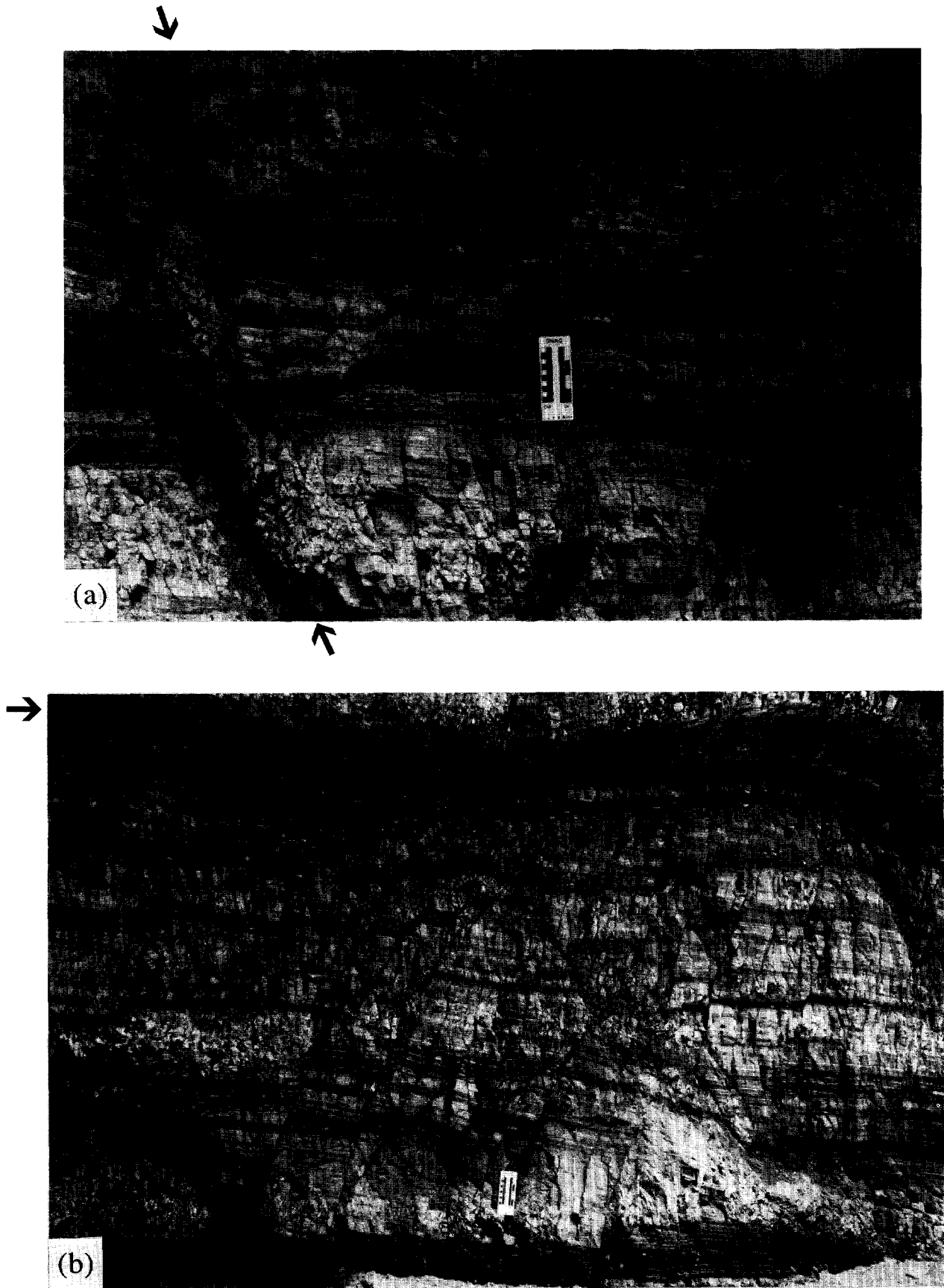


Fig. 5. (a) Photograph of faults at Section A. Note that small conjugate faults are confined to the laminated mudstone in the central portion of the photograph. Opal-CT beds are dragged and brecciated within the large fault found to the left (arrows). (b) Photograph of faults at Section C. The arrow marks the main clay detachment at the top of the measured section (bed #19).

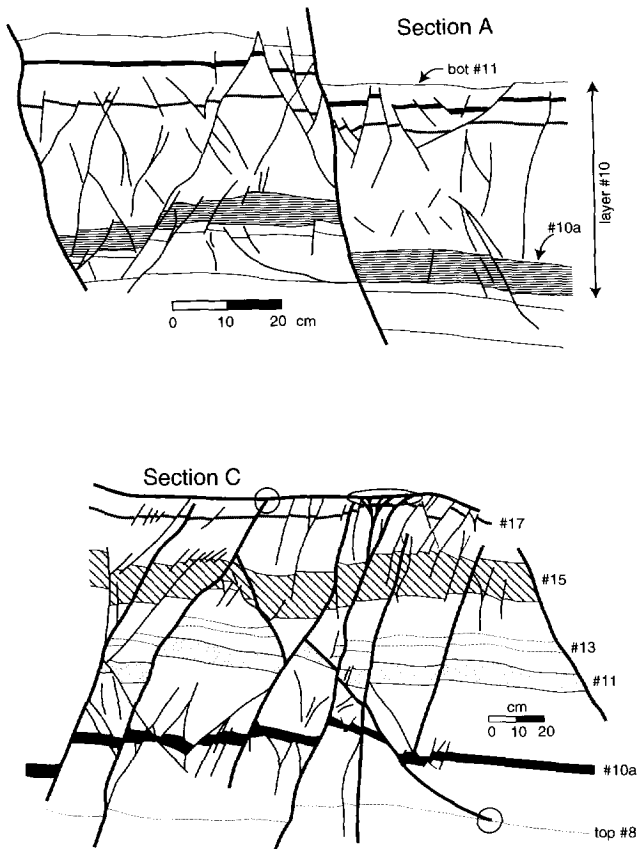


Fig. 6. Sketches of photographs in Fig. 5. Note how the large faults displace opal-CT horizons, and often merge and splay into bedding-plane detachments (circled areas).

## RESULTS

Plots of maximum dip separation versus fault length from Arroyo Burro Beach are presented in Fig. 7. Small faults from Sections A and C are plotted separately as their quantities are deemed sufficient for correlation (Fig. 7a & b). Data from all small faults are combined together in Fig. 7(c). A strong linear correlation ( $r^2 = 0.78$ ) exists between dip separation and length for small faults, which in all cases is stronger than the best logarithmic curve fit. Therefore,  $n = 1$  for small faults at Arroyo Burro, similar to results reported by other workers (Elliott, 1976; Opheim and Gudmundsson, 1989; Cowie and Scholz, 1992b; Dawers *et al.*, 1993; Clark and Cox, 1996; Schlische *et al.*, 1996). As is the case with most other studies, plots of small faults display considerable scatter (Walsh and Watterson, 1988; Cowie and Scholz, 1992b; Gillespie *et al.*, 1992; Cartwright *et al.*, 1995; Schlische *et al.*, 1996). The best linear fit for small faults shows that maximum offset across faults confined predominantly to mudstone intervals in the Monterey Formation is approximately one-tenth fault length, about three times greater than the ( $D/L$ ) ratio reported by Schlische *et al.* (1996) for small faults in massive siltstones. Nonetheless, faults at Arroyo Burro ranging from 1 to 70 cm in length

demonstrate a power law scaling relationship with regard to their dimensions.

In marked contrast to small faults, dip separation across large faults is independent of fault length as indicated by extremely low correlation coefficients for both linear and power law curve fits (Fig. 7d). The breakdown in  $D-L$  scaling relations is best seen in a plot where all data are combined together (Fig. 8). Note that small faults follow the best-fit linear trend, yet large faults deviate markedly when this line is extended into their range. Not only do many large faults plot far from their expected values based on a self-similar growth model, but the deviation is somewhat symmetrical, with large faults significantly falling both beneath and above the extrapolated relationship observed for small faults. In other words, many large faults have unusually small displacements relative to their lengths, whereas other large faults have anomalously large displacements. Large faults are subdivided into categories based on geometry and structural position, including isolated faults, faults that terminate in splays at detachments, faults that merge into detachments, faults resulting in dragged beds, and various combinations of these features (Fig. 8). We define isolated faults as those faults that extend across multiple beds but do not approach detachments.

## DISCUSSION

Displacements across normal faults at Arroyo Burro do not conform to a universal scaling relationship. Small faults less than 70 cm in length and confined to mudstone beds exhibit displacements that indeed correlate linearly with length. The  $D/L$  ratio of 0.11 for these small faults, though, is high relative to other ratios reported in the literature (Cowie and Scholz, 1992b; Schlische *et al.*, 1996). On the other hand, displacements associated with large faults cutting through multiple beds are independent of length, and their deviation from the expected scaling relation appears related to specific outcrop geometries, kinematics, and mechanical properties. In the following discussion we review proposed explanations for scatter in  $D-L$  plots and then present our theories for the breakdown in fault scaling relations at Arroyo Burro.

### *Proposed explanations for inconsistent fault scaling*

Numerous factors may contribute to the scatter and inconsistencies commonly observed in plots of fault displacement-length data, including errors associated with sampling effects and measurement biases (Walsh and Watterson, 1987, 1988; Cowie and Scholz, 1992b; Gillespie *et al.*, 1992), the influence of mechanical properties on fault growth (Walsh and Watterson, 1988; Cowie and Scholz, 1992a; Bürgmann *et al.*, 1994), and fault segment linkage and the temporal evolution of fault

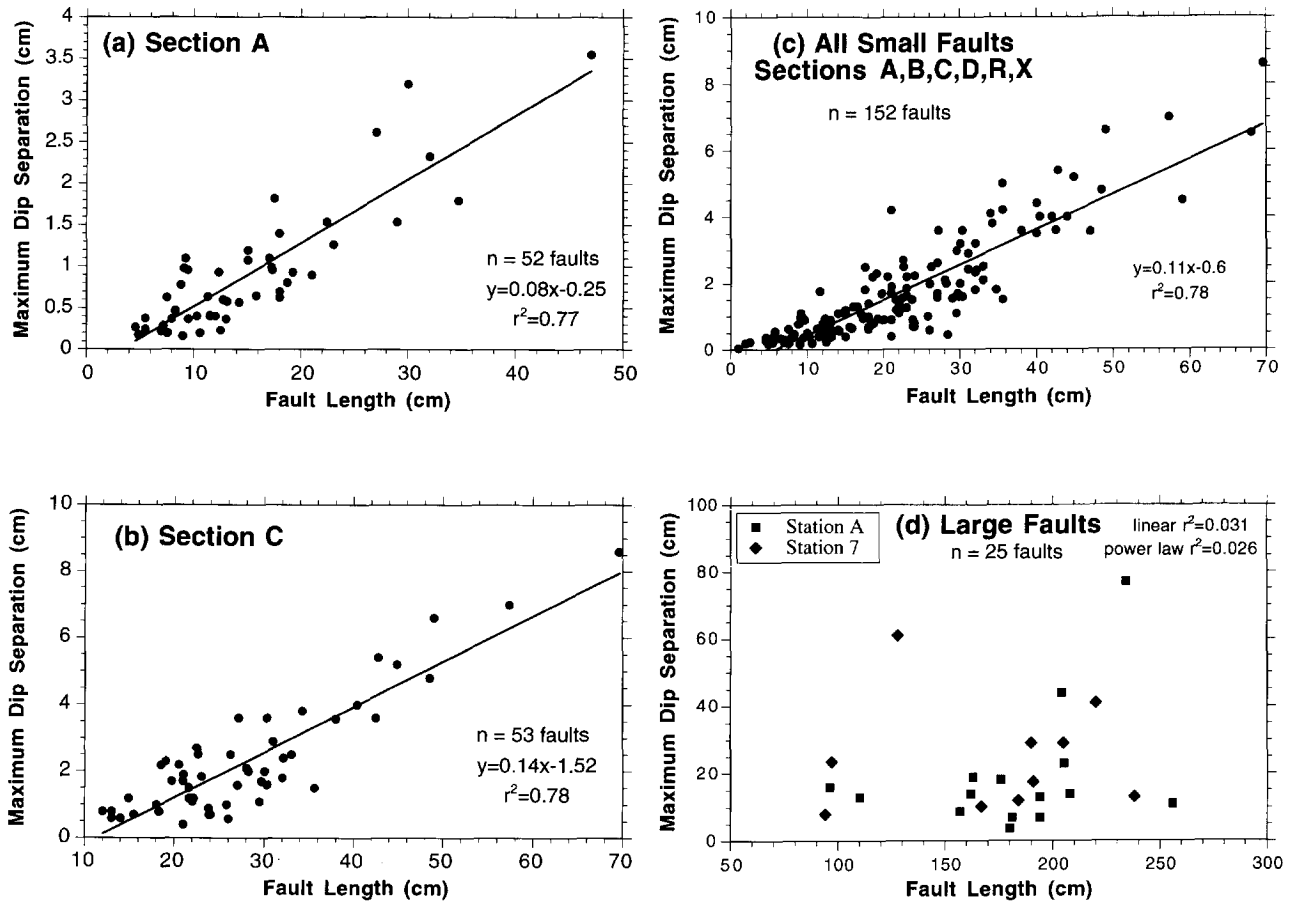


Fig. 7. Plots of maximum dip separation versus length for small and large faults at Arroyo Burro Beach.

systems (Peacock and Sanderson, 1991; Cartwright *et al.*, 1995; Willemse *et al.*, 1996; Wojtal, 1996).

Theoretical models for fault growth imply that displacement-length ratios should vary as a function of rock mechanical properties. For example, Walsh and Watter-

son (1988) propose that shear modulus is proportional to fault width and inversely proportional to the square root of displacement, whereas the Cowie and Scholz (1992a) model, based on post-yield fracture mechanics, suggests that  $D/L$  is proportional to the shear strength and inversely proportional to the shear modulus of the host rock. Effects of mechanical properties on fault growth are substantiated by field and seismic data, including the modification of fault displacement profiles (Muraoka and Kamata, 1983; Peacock, 1991) and the development of elliptical fault surfaces (Nicol *et al.*, 1996) due to mechanical layering.

Walsh and Watterson (1987) suggest that ‘ductile drag’ of incompetent beds can lead to consistently low displacement values along a fault profile. It is apparent from their discussion, however, that they are not referring to effects of frictional drag along the fault surface, but rather to the displacement of draped monoclinial flexures that develop in front of a propagating fault. Consequently, more competent beds that were not monoclinally flexed reveal true displacement, whereas low values of displacement derived from dragged beds represent a source of measurement error.

Both Peacock and Sanderson (1991) and Dawers and Anders (1995) report that individual fault segments within a larger fault zone display significantly greater  $D/L$  ratios than the composite linked fault zone and

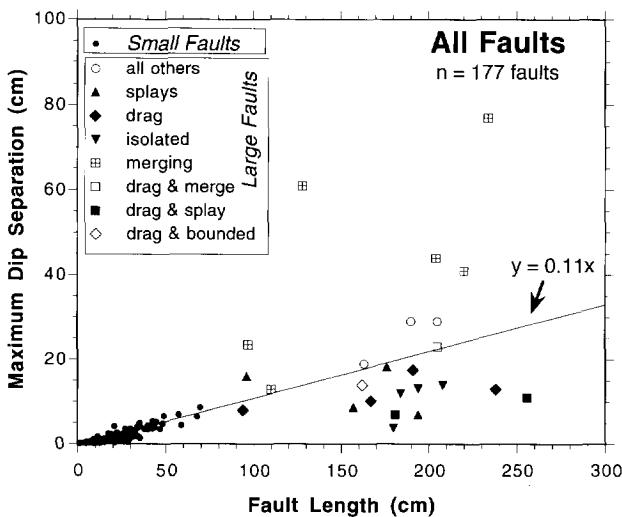


Fig. 8. Combined maximum dip separation-length plot for all normal faults at Arroyo Burro. Note that small faults follow a linear trend, but large faults do not. Large faults are divided into groups based on geometries and structural position.

adjacent isolated faults. In addition, Cartwright *et al.* (1995) hypothesize that scatter in  $D-L$  data from Canyonlands Graben, Utah and other data sets is due primarily to segment linkage during fault growth. Thus, the temporal evolution of a segmented fault system may contribute to changes and/or scatter in  $D-L$  plots. In a related study of fault displacement populations, Wojtal (1994, 1996) demonstrates that the kinematic evolution of a fault system through time results in a deviation from self-similarity; faults of different sizes exhibit different power law scaling relations. In the case of a contractional duplex system this change occurs when isolated thrust faults interact with bounding roof and floor thrusts (Wojtal, 1994), while for extensional faults this occurs when larger faults interact with each other or approach mechanical boundaries (Wojtal, 1996). As is the case with opening-mode veins (Gross and Engelder, 1995), mechanical layer thickness plays a critical role in controlling fracture scaling relations (Wojtal, 1996).

For the purpose of our discussion we distinguish between two kinds of fault linkage: the linkage of subparallel segments belonging to a composite fault zone, and the linkage of genetically different faults. In the former case, fault zones often evolve into a series of overlapping and interconnecting segments (Peacock, 1991; Peacock and Sanderson, 1991; Anders and Schlische, 1994; Childs *et al.*, 1995). Most segments of the fault zone are subparallel to each other, form in response to the same tectonic forces, and display similar kinematic development and sense of motion. Thus, fault segments and accommodating relay ramps combine to form a composite structure that in an overall sense reflects relatively uniform geometries and scaling relations (Dawers and Anders, 1995). In contrast, an example of the linkage of different faults would be the merging of a Mesozoic normal fault into a Paleozoic thrust detachment. A second example would be the linkage of an isolated, horse-confined thrust fault into a roof thrust, as outlined by Wojtal (1994). Even though these latter faults evolved together as part of the same system, their kinematics, geometries, and mechanics of formation are sufficiently different from each other to distinguish them from linked segments.

#### *Explanation for high $D/L$ ratios for small faults at Arroyo Burro*

A combination of geologic factors may have led to the  $D-L$  pattern observed at Arroyo Burro. In terms of lithology, field observations indicate that mechanical contrasts between mudstones and opal-CT porcellanites are quite large (Gross and Engelder, 1995). Our measurements of elastic properties for opal-CT beds from adjacent outcrops yield shear moduli of  $\sim 8$  GPa. We were unable to measure properties of the mudstone due to its friable nature, however a qualitative mechanical analysis implies it is an extremely weak lithology (Gross, 1995), and we suspect its shear modulus is less than

1 GPa. In the fault growth model of Walsh and Watterson (1988), a low shear modulus would lead to a high  $D/L$  ratio. For the model proposed by Cowie and Scholz (1992a), the predicted relationship is less clear because  $D/L$  depends on two material properties, namely the shear strength and shear modulus of the rock. Because the grade of silica diagenesis implies a maximum burial depth of 3 km for the Monterey Formation at Arroyo Burro (Isaacs, 1982; Gross, 1995), confining stress ( $< 50$  MPa), and hence shear strengths of the rock layers, are relatively low ( $< 150$  MPa). For relatively small differences in shear strength, the Cowie and Scholz (1992a) model suggests that large differences in shear modulus would result in a wide range of  $D/L$  ratios, with higher ratios corresponding to lower moduli. Thus, the high  $D/L$  ratio of 0.11 observed for small faults at Arroyo Burro may be attributed to the weak mechanical properties of mudstone beds.

#### *Explanation for large fault $D-L$ results*

Displacement across large faults apparently is not related to length, as inferred from visual inspection of plots as well as the lack of correlation for linear and power law curve fits (Figs 7d & 8). Field observations indicate that several faults are segmented, though a majority of both small and large faults are not segmented. Furthermore, we do not observe a difference in degree of segmentation between small and large faults. Segmentation may lead to increased scatter in  $D-L$  plots (Dawers and Anders, 1995), however, it should not result in a lack of correlation (Cartwright *et al.*, 1995). Therefore, we conclude that some of the scatter in  $D-L$  plots for both small and large faults may be attributable to fault segment linkage, but this process is not responsible for the breakdown that occurs when faults extend beyond mudstone beds.

Large faults may display anomalously high or low displacements with respect to the extrapolated linear trend derived from small faults. As large faults grow beyond the confines of weak mudstone layers and cut across more competent opal-CT beds, the mechanical properties of rock (both local and integrated over the entire fault length) encountered by the fault change dramatically. According to theoretical considerations described above, the sharp increase in shear modulus would result in a decrease in  $D/L$  (Walsh and Watterson, 1988; Cowie and Scholz, 1992a). Furthermore, numerical models of Bürgmann *et al.* (1994) demonstrate that an inclusion of high modulus material in a low modulus rock should decrease fault displacement with respect to its length (Fig. 9). At Arroyo Burro, these high modulus inclusions encountered by large faults are opal-CT beds, which have estimated shear moduli approximately 10 times greater than the mudstones. The effect on the  $D-L$  relationship of cutting across beds with higher moduli should best be observed for isolated faults, which are large faults that displace opal-CT beds yet terminate

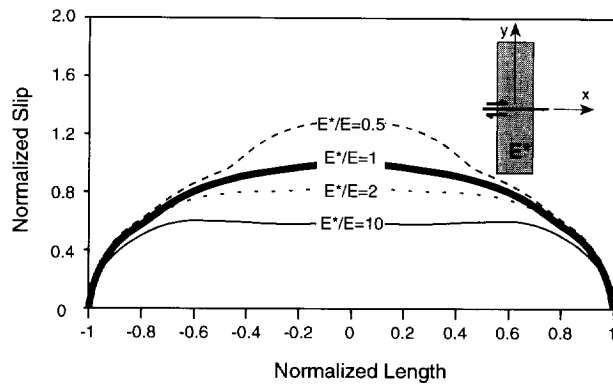


Fig. 9. Effect of an inclusion with different Young's modulus from the host material on fault displacement profiles, from numerical models of Bürgmann *et al.* (1994).  $E^*/E$  is the ratio of Young's modulus in the inclusion to that in the host. Note that a fault encountering an inclusion of higher modulus (e.g. a fault encountering opal-CT beds within a mudstone unit) will result in a decrease in displacement relative to fault length.

prior to reaching detachments. As seen in Fig. 8, all large faults that fall into this category plot below the  $y = 0.11x$  line as expected — evidence that mechanical properties exhibited by different lithologies influence fault growth at Arroyo Burro.

Another potential factor that may affect the  $D/L$  ratio is frictional drag of opal-CT beds, which occurred adjacent to a number of large faults. It is clear that the 'ductile drag' process described by Walsh and Watterson (1987) is not responsible for drag observed at Arroyo Burro, as monoclin folds are not found near fault tips, and drag may be observed along the entire fault length. In contrast, strong evidence for a frictional origin includes intense brecciation and block rotation within dragged zones of opal-CT beds. Analytical and numerical models suggest that any increase in frictional resistance would lead to a decrease in the  $D/L$  ratio (see eq. 5 and fig. 5b of Bürgmann *et al.*, 1994). Faults characterized solely by dragged opal-CT beds fall beneath the extrapolated line, implying that frictional resistance of competent beds at Arroyo Burro reduces maximum displacement across large faults.

We now turn our attention to effects of fault termination geometry, kinematics, and temporal evolution of the overall fault system at Arroyo Burro. Large faults are presently at different stages of development, ranging from isolated to fully merged with bedding plane detachments. Although precise timing of extensional faulting with respect to development of flexural slip folding is unresolved, it is probable that initiation of normal faulting in mudstone beds (i.e. small faults) occurred in conjunction with flexural slip, as both structural elements are related to the same folding event (Fig. 10a). However, it is abundantly clear that bedding plane detachments were active prior to the development of large faults (i.e. prior to the extension of small faults beyond the confines of individual mudstone beds), as large faults abut against, splay, and merge into slip

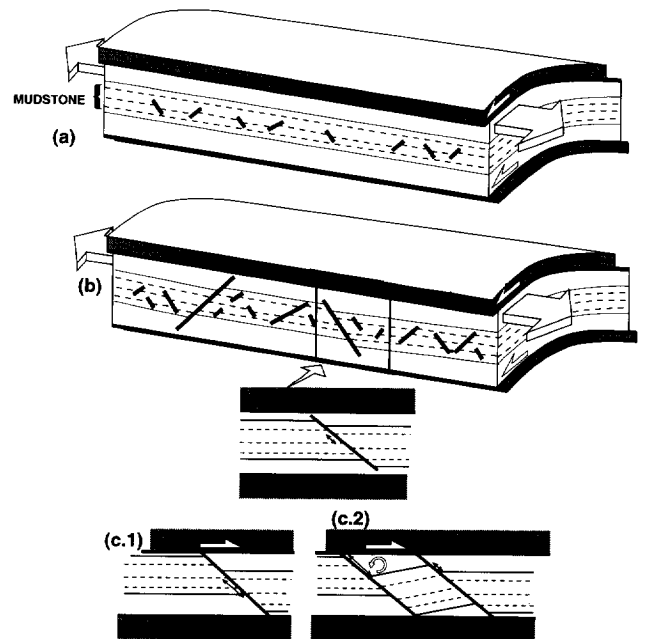


Fig. 10. Kinematic model for temporal development of normal faults at Arroyo Burro. (a) Small faults grow in mudstone beds to accommodate axis-parallel extension during multi-layer flexural slip folding. (b) Several small faults grow into large faults by extending beyond confines of mudstone beds. (c) Examples of large faults eventually merging into bedding parallel detachments, allowing for continued displacement to occur without an increase in length as slip is transferred to the detachment.

horizons (Fig. 3). Splays at Arroyo Burro occur due to mechanical interaction of large faults as they approach detachment surfaces, and may develop in one of two ways. In the first case (Case 1 of Fig. 11) several splays branch off a large fault. Displacement across each individual splay is transferred to the large fault, such that the maximum displacement observed across the fault reflects the sum of displacement across the large fault plus displacements across all of the splays. This would result in an increase in  $D/L$  for the large fault. In the second case (Case 2 of Fig. 11) fault splays originate near the detachment interface and propagate towards the large fault, eventually merging with the large fault. Splays act as isolated individual faults, thus displacement would not be transferred from splays to a large fault because the contact points mark intersections of tip lines with zero displacement. Thus, the geometry of the latter case would lead to a decrease in  $D/L$ . The sketch of Fig. 3 shows faults with splay zones at various stages of development. Several currently developing splay zones display a growth pattern resembling Case 1 (e.g. top of large fault in left side of section A) while others reflect Case 2 (e.g. the large fault in the left side of sections C and R). Splayed faults plot above, beneath and near the line of  $y = 0.11x$  in Fig. 8, perhaps because splays can result in either a decrease or increase in  $D/L$  depending upon how they develop.

Once large normal faults merge into bedding parallel slip zones, continued displacement can occur without

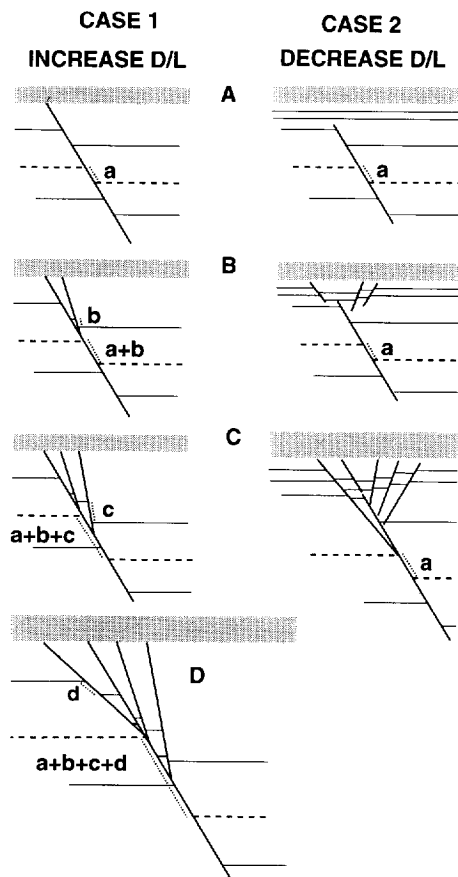


Fig. 11. Effect of splay development at the ends of large faults on  $D/L$  ratios. Both types of splay development occur at Arroyo Burro. See text for more details.

increasing fault length by the transfer of displacement to the detachment through branch lines (Fig. 10c). At this point, fault blocks are free to rotate, and antithetic block rotation within a simple shear zone (Jordan, 1991) indeed occurs at Arroyo Burro, as shown schematically in Fig. 12. Displacement across merged faults increases while

fault length (i.e. the distance between branch lines) remains unchanged, and blocks rotate independently of each other. Consequently, magnitude of displacement and amount of block rotation can vary dramatically from one fault to the next. The effect of large faults merging into detachments is to increase  $D/L$ , and all of the merged normal faults at Arroyo Burro plot on or above the extrapolated line (Fig. 8). Thus, as Wojtal (1994) demonstrated for fault displacement populations in thrust duplexes, displacement-length scaling of large faults at Arroyo Burro is influenced by the change in kinematics that occurs during the temporal development of a fault system.

*Arroyo Burro data within context of other studies*

Although numerous workers debate the appropriateness of combining  $D-L$  data sets, the tendency to group different studies together over many orders of magnitude remains strong (Walsh and Watterson, 1988; Marrett and Allmendinger, 1991; Cowie and Scholz, 1992b; Gillespie *et al.*, 1992; Schlische *et al.*, 1996). This has been primarily driven by desires to prove self-similarity, determine the true value of the power law coefficient ( $n$ ), and to evaluate the appropriateness of fault growth models. However, logarithmic plots, though convenient for plotting data over many orders of magnitude, tend to mask true differences between data sets. Theoretical and numerical models suggest that rock mechanical properties, applied tectonic forces, and strain should affect  $D/L$  ratios (Walsh and Watterson, 1988; Cowie and Scholz, 1992a; Bürgmann *et al.*, 1994). The temporal development of a fault system, whether through segment linkage or merging with other structures, also exerts an influence on fault displacement (Wojtal, 1994, 1996; Dawers and Anders, 1995). Even the apparently simple issue of defining fault dimensions poses a dilemma: whereas some workers define length ( $L$ ) as the fault dimension

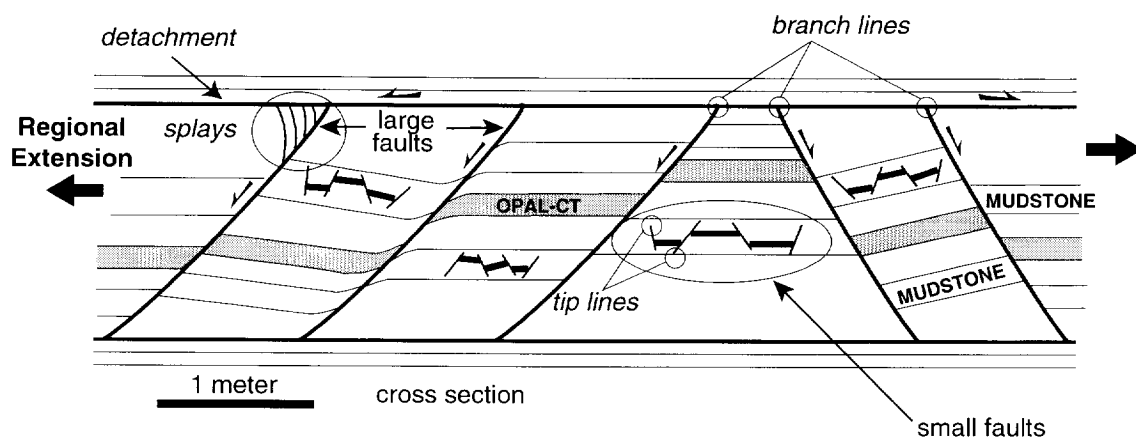


Fig. 12. Schematic diagram depicting effects of mechanical stratigraphy and kinematics on fault development and displacement. Small conjugate normal faults are confined to mudstone beds and terminate as tip lines. Large faults eventually merge into detachments, allowing for the rotation of fault-bounded blocks and thus an increase in displacement relative to length. Fault splays, dragged beds, and differences in mechanical properties also affect  $D/L$ .

parallel to slip and width as the dimension normal to slip (Muraoka and Kamata, 1983; Walsh and Watterson, 1988; Gillespie *et al.*, 1992), others define length as the dimension parallel to fault strike, regardless of sense of motion (Cowie and Scholz, 1992a,b; Dawers *et al.*, 1993; Cartwright *et al.*, 1995; Schlische *et al.*, 1996). Because mechanical layering often results in elliptical fault surfaces (Nicol *et al.*, 1996), inconsistencies in defining fault length may lead to ratios that differ by a factor of ten. In the most rigorous statistical analysis to date, Clark and Cox (1996) demonstrate that most data sets conform to a linear relationship between fault displacement and length (i.e.  $n=1$ ), though slopes differ among individual data sets. The differences in slope may in part reflect the unique geologic conditions at each locality.

Our data from faults at Arroyo Burro support the hypotheses proposed by Wojtal (1994, 1996) and Bürgmann *et al.* (1994) that variations in mechanical properties due to rock layering as well as the temporal evolution of a fault system will result in deviations from self-similarity. Rather than a change in scaling relationship observed by Wojtal for fault displacement populations, we observe a complete breakdown in the linear  $D-L$  relationship for large faults at Arroyo Burro. We attribute this lack of correlation to a combination of geologic factors that can be identified through careful field observations. Propagation of faults into beds of higher elastic moduli, as well as frictional drag reduces the  $D/L$  ratio. Splays as faults approach detachment surfaces can either increase or decrease  $D/L$  ratios depending upon how they developed. Once large faults merge into bedding plane detachments a kinematic change occurs as they accommodate block rotation within a simple shear zone, leading to high  $D/L$  ratios. We speculate that the latter process may in part be responsible for the breakdown in linear scaling for faults reported by Cartwright *et al.* (1995), which occurs at a length of  $\sim 1$  km and thus a radius of  $\sim 500$  m, approximately equal to depth to a major evaporitic detachment (see figs 2 & 3 in Cartwright *et al.*, 1995). Based on our observations at Arroyo Burro, we conclude that  $D/L$  ratios are strongly influenced by local geologic factors, and consequently we believe the geologic significance of analyzing combined global data sets remains unresolved.

Displacement across faults and the development of fault systems are greatly influenced by mechanical stratigraphy; the magnitude of strain and the manner in which strain is accommodated often depend upon lithology and pre-existing structural discontinuities (Gross and Engelder, 1995; Wojtal, 1996). Furthermore, contrasts in lithology often control the mechanical and kinematic development of fault systems, as for example the localization of detachments in incompetent units and the development of thrust ramps in more competent layers (Boyer and Elliott, 1982; Eisenstadt and DePaor, 1987). One effect of mechanical stratigraphy is to confine structures to individual units, thereby proportionally

restricting their dimensions to mechanical layer thickness (Narr and Suppe, 1991; Gross, 1993; Wojtal, 1994, 1996; Gross and Engelder, 1995; Marrett, 1996). Because mechanical layer thicknesses can range at least from millimeters to kilometers, we prefer defining 'small' versus 'large' faults relative to the thickness of the mechanical layer in question. At Arroyo Burro, the critical thicknesses are: (1) individual mudstone beds  $< 70$  cm where faults are confined to a single weak lithology; and (2) packages of multiple beds 0.8–3 m thick bounded by bedding plane detachments.

## CONCLUSIONS

Small faults confined to mudstone beds at Arroyo Burro Beach, California display a linear correlation between displacement and length, with the relatively high  $D/L$  ratio attributable to a low shear modulus for mudstone. In contrast, displacement across larger faults that extend across multiple beds is independent of length. Non-coincidentally, the breakdown in fault scaling occurs precisely at the point where fault dimensions exceed maximum mudstone bed thickness.

The lack of correlation between displacement and length for large faults arises from a number of local geologic factors related to lithology and tectonic history of rocks exposed at Arroyo Burro Beach, including mechanical properties, fault geometries and kinematics, and the temporal evolution of a flexural slip fold extending parallel to its hinge. The propagation of faults into neighboring, more competent opal-CT beds reduces  $D/L$ , as does the effect of frictional drag. Splays at the end of large faults can either reduce or increase displacement relative to length, depending upon how they form. Large faults that merge into detachments can continue to accommodate displacement during block rotation while their lengths remain constant, resulting in high  $D/L$ .

Regional tectonic forces superimposed onto the lithologically heterogeneous Monterey Formation led to the development of a fault system whose growth was locally controlled by mechanical stratigraphy and structural style. Once faults extended beyond the confines of mudstone beds, fault growth was influenced by numerous geologic factors such that displacement no longer correlates with length. Thus, large faults at Arroyo Burro do not propagate as if in a homogeneous medium according to a universal growth model. Because lithologic diversity and structural complexity will vary among rock types and tectonic environments, we emphasize the importance of characterizing the influence of local mechanical anisotropies and deformation styles on fault development.

*Acknowledgements*—We benefited greatly from discussions with Rolf Ackermann, Wendy Bartlett, Alexander Becker, and Grenville Draper. Thoughtful reviews by Trenton Cladouhos, Nancye Dawers, and Steven Wojtal greatly improved the manuscript. Acknowledgement is made to the Donors of The Petroleum Research Fund, administered by the

American Chemical Society for the support of this research through PRF Grant 28338-GB2, and to the Government of Spain DGICYT Grant PB-93-1149 C03-02.

## REFERENCES

- Anders, M. H. and Schlische, R. W. (1994) Overlapping faults, intrabasin highs, and the growth of normal faults. *Journal of Geology* **102**, 165–180.
- Boyer, S. E. and Elliott, D. (1982) Thrust systems. *American Association of Petroleum Geologists Bulletin* **66**, 1196–1230.
- Bramlette, M. N. (1946) The Monterey Formation of California and the origin of its siliceous rocks. *Professional Paper U.S. Geological Survey* **212**, 57.
- Bürgmann, R., Pollard, D. D. and Martel, S. J. (1994) Slip distributions on faults: effects of stress gradients, inelastic deformation, heterogeneous host-rock stiffness, and fault interaction. *Journal of Structural Geology* **16**, 1675–1690.
- Cartwright, J. A., Trudgill, B. D. and Mansfield, C. S. (1995) Fault growth by segment linkage: an explanation for scatter in maximum displacement and trace length data from the Canyonlands Grabens of SE Utah. *Journal of Structural Geology* **17**, 1319–1326.
- Childs, C., Watterson, J. and Walsh, J. J. (1995) Fault overlap zones within developing normal fault systems. *Journal of geological Society London* **152**, 535–549.
- Cladouhos, T. T. and Marrett, R. (1996) Are fault growth and linkage models consistent with power-law distributions of fault lengths? *Journal of Structural Geology* **18**, 281–293.
- Clark, R. M. and Cox, S. J. D. (1996) A modern regression approach to determining fault displacement–length scaling relationships. *Journal of Structural Geology* **18**, 147–154.
- Cowie, P. A. and Scholz, C. H. (1992a) Physical explanation for the displacement–length relationship of faults using a post-yield fracture mechanics model. *Journal of Structural Geology* **14**, 1133–1148.
- Cowie, P. A. and Scholz, C. H. (1992b) Displacement–length scaling relationships for faults: data synthesis and discussion. *Journal of Structural Geology* **14**, 1149–1156.
- Crouch, J. K. (1979) Neogene tectonic evolution of the California Continental borderland and western Transverse Ranges. *Geological Society of America Bulletin* **90**, 338–345.
- Dawers, N. H. and Anders, M. H. (1995) Displacement–length scaling and fault linkage. *Journal of Structural Geology* **17**, 607–614.
- Dawers, N. H., Anders, M. H. and Scholz, C. H. (1993) Growth of normal faults: displacement–length scaling. *Geology* **21**, 1107–1110.
- Eisenstadt, G. and DePaor, D. G. (1987) Alternative model of thrust-fault propagation. *Geology* **15**, 630–633.
- Elliott, D. (1976) Energy balance and deformation mechanisms of thrust sheets. *Philosophical Transactions Royal Society London* **A283**, 289–312.
- Gillespie, P. A., Walsh, J. J. and Watterson, J. (1992) Limitations of dimension and displacement data from single faults and the consequences for data analysis and interpretation. *Journal of Structural Geology* **14**, 1157–1172.
- Gross, M. R. (1993) The origin and spacing of cross joints: examples from the Monterey Formation Santa Barbara coastline, California. *Journal of Structural Geology* **15**, 737–751.
- Gross, M. R. (1995) Fracture partitioning: failure mode as a function of lithology in the Monterey Formation of coastal California. *Geological Society of America Bulletin* **107**, 779–792.
- Gross, M. R. and Engelder, T. (1995) Strain accommodated by brittle failure in adjacent units of the Monterey Formation, U.S.A.: scale effects and evidence for uniform displacement boundary conditions. *Journal of Structural Geology* **17**, 1303–1318.
- Hornafius, S. J. (1985) Neogene tectonic rotation of the Santa Ynez Range, Western Transverse Ranges, California, suggested by paleomagnetic investigation of the Monterey Formation. *Journal of geophysical Research* **90**, 12,503–12,522.
- Hull, J. (1988) Thickness–displacement relationships for deformation zones. *Journal of Structural Geology* **10**, 431–435.
- Isaacs, C. M. (1980) Diagenesis in the Monterey Formation examined laterally along the coast near Santa Barbara, California. Unpublished Ph.D. thesis, Stanford University, Stanford, California.
- Isaacs, C. M. (1982) Influence of rock composition on kinetics of silica phase changes in the Monterey Formation Santa Barbara area, California. *Geology* **10**, 304–308.
- Isaacs, C. M. (1983) Compositional variation and sequence in the Miocene Monterey Formation, Santa Barbara coastal area California. In *Cenozoic Marine Sedimentation, Pacific Margin, U.S.A.*, eds D. K. Lane and R. J. Steel. *Pacific Section Society of Economic Paleontologists and Mineralogists Special Publication*, 117–132.
- Jordan, P. G. (1991) Development of asymmetric shale pull-aparts in evaporite shear zones. *Journal of Structural Geology* **13**, 399–409.
- Luyendyk, B. P., Kamerling, M. J., Terres, R. R. and Hornafius, S. J. (1985) Simple shear of southern California during Neogene time suggested by paleomagnetic declinations. *Journal of geophysical Research* **90**, 12454–12466.
- Marrett, R. (1996) Aggregate properties of fracture populations. *Journal of Structural Geology* **18**, 169–178.
- Marrett, R. and Allmendinger, R. W. (1991) Estimates of strain due to brittle faulting: sampling of fault populations. *Journal of Structural Geology* **13**, 735–738.
- Marrett, R. and Allmendinger, R. W. (1992) Amount of extension on 'small' faults: An example from the Viking graben. *Geology* **20**, 47–50.
- Muraoka, H. and Kamata, H. (1983) Displacement distribution along minor fault traces. *Journal of Structural Geology* **5**, 483–495.
- Murata, K. J. and Larson, R. R. (1975) Diagenesis of Miocene siliceous shales, Temblor Range California. *U.S. Geological Survey Journal of Research* **3**, 553–556.
- Namson, J. and Davis, T. (1988) Structural transect of the western Transverse Ranges, California: Implications for lithospheric kinematics and seismic risk evaluation. *Geology* **16**, 675–679.
- Narr, W. and Suppe, J. (1991) Joint spacing in sedimentary rocks. *Journal of Structural Geology* **13**, 1037–1048.
- Nicol, A., Watterson, J., Walsh, J. J. and Childs, C. (1996) The shapes, major axis orientations and displacement patterns of fault surfaces. *Journal of Structural Geology* **18**, 235–248.
- Opheim, J. A. and Gudmundsson, A. (1989) Formation and geometry of fractures, and related volcanism, of the Krafla fissure swarm, northeast Iceland. *Geological Society of America Bulletin* **101**, 1608–1622.
- Peacock, D. C. P. (1991) Displacement and segment linkage in strike-slip fault zones. *Journal of Structural Geology* **13**, 1025–1035.
- Peacock, D. C. P. and Sanderson, D. J. (1991) Displacements, segment linkage and relay ramps in normal fault zones. *Journal of Structural Geology* **13**, 721–733.
- Pisciotta, K. A., and Garrison, R. E. (1981) Lithofacies and depositional environments of the Monterey Formation, California. In *The Monterey Formation and Related Siliceous Rocks of California*, eds R. E. Garrison, R. G. Douglas, K. E. Pisciotta, C. M. Isaacs and J. C. Ingle. *Pacific Section Society of Economic Paleontologists and Mineralogists Special Publication*, 97–122.
- Schlische, R. W., Young, S. S., Ackermann, R. V. and Gupta, A. (1996) Geometry and scaling relations of a population of very small rift-related normal faults. *Geology* **24**, 683–686.
- Scholz, C. H. and Cowie, P. A. (1990) Determination of total strain from faulting using slip measurements. *Nature* **346**, 837–839.
- Shaw, J. H. and Suppe, J. (1994) Active faulting and growth folding in the eastern Santa Barbara Channel, California. *Geological Society of America Bulletin* **106**, 607–626.
- Sibson, R. H. (1996) Structural permeability of fluid-driven fault–fracture meshes. *Journal of Structural Geology* **18**, 1031–1042.
- Walsh, J. J. and Watterson, J. (1987) Distributions of cumulative displacement and seismic slip on a single normal fault surface. *Journal of Structural Geology* **9**, 1046–1093.
- Walsh, J. J. and Watterson, J. (1988) Analysis of the relationship between displacements and dimensions of faults. *Journal of Structural Geology* **10**, 239–247.
- Walsh, J., Watterson, J. and Yielding, G. (1991) The importance of small-scale faulting in regional extension. *Nature* **351**, 391–393.
- Willemsse, E. J. M., Pollard, D. D. and Aydin, A. (1996) Three-dimensional analyses of slip distributions on normal fault arrays with consequences for fault scaling. *Journal of Structural Geology* **18**, 295–309.
- Wojtal, S. F. (1994) Fault scaling laws and the temporal evolution of fault systems. *Journal of Structural Geology* **16**, 603–612.
- Wojtal, S. F. (1996) Changes in fault displacement populations correlated to linkage between faults. *Journal of Structural Geology* **18**, 265–279.
- Yeats, R. S. (1983) Large-scale Quaternary detachments in Ventura basin, southern California. *Journal of geophysical Research* **88**, 569–583.